Chinese Chemical Letters 35 (2024) 109929

Contents lists available at ScienceDirect

Chinese Chemical Letters

journal homepage: www.elsevier.com/locate/cclet

Responsive organic room-temperature phosphorescence materials for spatial-time-resolved anti-counterfeiting

Jiayin Zhou[a,b,1], Depeng Liu[a,b,1], Longqiang Li[a,b], Min Qi[a,b], Guangqiang Yin[a,b,*], Tao Chen[a,b,c,*]

[a] Key Laboratory of Advanced Marine Materials, Ningbo Institute of Materials Technology and Engineering, Chinese Academy of Sciences, Ningbo 315201, China
[b] School of Chemical Sciences, University of Chinese Academy of Sciences, Beijing 100049, China
[c] College of Material Chemistry and Chemical Engineering, Key Laboratory of Organosilicon Chemistry and Material Technology, Ministry of Education, Hangzhou Normal University, Hangzhou 311121, China

ARTICLE INFO

Article history:
Received 26 March 2024
Revised 23 April 2024
Accepted 26 April 2024
Available online 27 April 2024

Keywords:
Room-temperature phosphorescence
pH-responsive
Hydrogen bonding interactions
Spatial-time-resolved anti-counterfeiting
Terpyridine

ABSTRACT

Stimulus-responsive room-temperature phosphorescence (RTP) materials have gained significant attention for their important optoelectronic application prospects. However, the fabrication strategy and underlying mechanism of stimulus-responsive RTP materials remain less explored. Herein, we present a reliable strategy for achieving pH-responsive RTP materials by integrating poly(vinyl alcohol) (PVA) with carboxylic acid or amino group functionalized terpyridine (Tpy) derivatives. The resulting Tpy derivatives-based RTP materials displayed reversible changes in emission color, intensity, and lifetime of both prompt and delayed emission. Notably, the RTP emission undergoes a significant diminish upon exposure to acid due to the protonation of Tpy units. Taking advantage of the decent RTP emission and pH-responsiveness of these RTP films, a spatial-time-resolved anti-counterfeiting application is demonstrated as a proof-of-concept for largely enhancing the security level. This study not only provides new prospects for developing smart RTP materials but also promotes the advancement of optical anti-counterfeiting applications.

Organic room-temperature phosphorescence (RTP) is a fascinating optical phenomenon that originates from tardy radiation from the excited triplet state to the ground state under ambient conditions [1–5]. In comparison with inorganic counterparts, organic RTP materials reveal plenty of advantages including low cost, abundant chemical design, mild preparation conditions, ease of processing and low biotoxicity [6–11]. However, the low spin-orbit coupling (SOC) and severe nonradiative transition of organic luminogens make it highly difficult to realize purely organic RTP emission. In addressing these challenges, several effective strategies have been well established to achieve organic RTP materials primarily based on enhancing SOC and suppressing nonradiative dissipation. Generally, the introduction of heavy atoms (Cl, Br, I) and heteroatoms (N, S, P) with lone pair electrons proved to be a powerful way to enhance SOC for promoting the forbidden transition of intersystem crossing (ISC) [12]. For another, rigid microenvironments can be created by crystallization [13–15], polymerization [16–19], host-guest system [8,20–26], aggregation [27–32], and so on [33–35], facilitating the stabilization of triplet excitons to access long-lived RTP materials. These molecular design and construction strategies have greatly advanced the development of organic RTP materials.

In recent years, stimulus-responsive RTP materials have attracted considerable attention owing to their great promise in a wide variety of applications including information encryption, anti-counterfeiting, and chemical sensing [36–39]. Importantly, the optical properties of stimulus-responsive RTP materials such as emission wavelength, intensity and lifetime can be well regulated by external stimuli such as pH [40–46], light [23,47,48], heat [49,50], humidity [51,52], mechanical force [53–57]. For instance, Zhang and coauthors presented a series of acid-responsive RTP materials demonstrating that strong RTP emission of organic phosphors could be turned on upon acid treatment [42]. Recently, Li and coauthors reported a capture-release strategy for constructing reversible stimulus-responsive RTP materials by regulating the formation and dissociation of B-N bonds, revealing great potential in information storage and anti-counterfeiting [40]. In comparison with static RTP materials, those stimulus-responsive RTP materials have distinctive advantages of dynamic variations and more

* Corresponding authors.
E-mail addresses: yinguangqiang@nimte.ac.cn (G. Yin), tao.chen@nimte.ac.cn (T. Chen).
[1] These authors contributed equally to this work.

https://doi.org/10.1016/j.cclet.2024.109929
1001-8417/

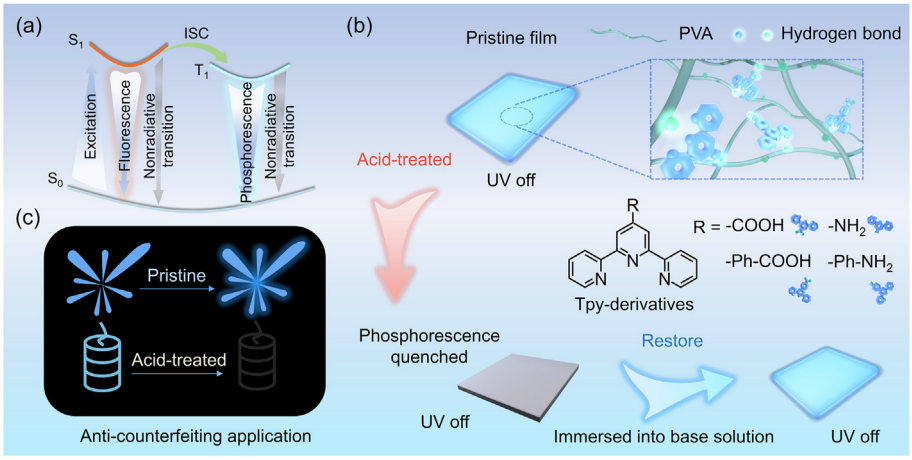

Scheme 1. (a) Simplified Jablonski diagram of RTP emission. (b) Schematic illustration of pH-responsive RTP films and their reversible pH-responsiveness. (c) Anti-counterfeiting application of pH-responsive RTP films.

abundant optical tunability. Furthermore, different from stimulus-responsive fluorescence materials, the stimulus-responsive RTP materials are capable of providing an additional time scale for related applications. Although they are highly promising in optoelectronic applications, only few examples of stimulus-responsive RTP materials have been reported so far. The related fabrication strategy and underlying mechanism remain less explored.

In this study, we present a feasible method for achieving pH-responsive RTP materials by integrating poly(vinyl alcohol) (PVA) with carboxylic acid or amino group functionalized terpyridine (Tpy) derivatives (Scheme 1). Wherein the carboxylic acid and amino groups act as both hydrogen bond donor and acceptor for enhancing hydrogen bonding interactions between organic phosphors and PVA. For one, the heteroatoms of these Tpy derivatives are beneficial to enhancing spin−orbit coupling (SOC) between excited singlet and triplet states [12]. For another, the Tpy unit provides an excellent platform for realizing pH-responsiveness owing to its reversible protonation and deprotonation upon exposure to acid and base, respectively. As our expected, the RTP properties of these Tpy derivatives-based films exhibit a significant degradation upon exposure to acid due to the protonation of Tpy units. On the contrary, the lifetimes of RTP films reveal a slight prolongation when exposed to base solution. Based on the decent RTP performance and pH-responsiveness of these Tpy derivatives-based films, a spatial-time-resolved anti-counterfeiting application is demonstrated with greatly enhanced security level.

In order to prepare pH-responsive RTP materials, four Tpy-derivatives denoted by Tpy-COOH, Tpy-Ph–COOH, Tpy-NH_2, and Tpy-Ph–NH_2, respectively, were rationally selected as organic phosphors (Fig. 1). The pH-responsive RTP films were facilely fabricated by integrating Tpy-derivatives with PVA matrix, followed by drop-casting and thermal annealing processes. In the first step, a clear and homogeneous precursor solution was obtained by stirring a mixture of Tpy-derivatives and PVA at 96 °C for 50 min. After drying at 30 °C for 5 h and then heating at 60 °C for 0.5 h, transparent PVA-Tpy-derivatives RTP films were achieved successfully. Thereafter, UV–vis absorption, steady-state and time-resolved photoluminescent properties of PVA-Tpy-derivatives RTP films were fully studied as displayed in Fig. 1. Obviously, the maximum absorption peaks of these RTP films are all located at around 280 nm, which can be assigned to the strong absorption of Tpy group [58]. The fluorescence spectrum of PVA-Tpy-COOH film exhibits dual emission at around 360 nm and 470 nm accompanied by an intense delayed emission at 470 nm. After fitting analysis, the average lifetime of the RTP emission at 470 nm is measured to be 339.12 ms, manifesting a long-lived feature. The PVA-Tpy-Ph–COOH film reveals similar optical features with those of PVA-Tpy-COOH film, except for considerable prolongation of lifetime up to 397.93 ms. Differently, the prompt emission of PVA-Tpy-NH_2 film displays a dominating emission at 377 nm. The delayed emission is centered at around 450 nm along with an ultralong lifetime of up to 471.10 ms. In comparison with PVA-Tpy-NH_2 film, the prompt emission of PVA-Tpy-Ph–NH_2 film undergoes an obvious red-shift to 441 nm ascribed to the extension of π-conjugation. Accordingly, the delayed emission of PVA-Tpy-Ph–NH_2 film is redshifted to 493 nm, showing intense springgreen afterglow. Notably, the PVA-Tpy-Ph–NH_2 film exhibits longest lifetime of up to 696.33 ms compared with the other three composite films. In sharp contrast to these PVA-based materials, the powders of these four organic phosphors exhibit poor optical performances without visible afterglow emission (Fig. S1 in Supporting information). These results demonstrate that ultralong RTP emission can be successfully achieved via the introduction of Tpy derivatives into PVA matrix.

Considering the doping concentration of organic phosphors may have an influence on the photophysical properties, a series of films with different doping concentration (0.025–0.4 wt%) were prepared. As shown in Fig. S2 (Supporting information), these pH-responsive RTP films all display high transparency, particularly for PVA-Tpy-COOH and PVA-Tpy-NH_2 films showing more than 90 % of transmittance in the visible region. However, the RTP films of PVA-Tpy-COOH and PVA-Tpy-NH_2 get a little opaque when the doping concentration exceeds 0.2 wt%. In addition, the UV-absorbance of these films undergo a significant increase along with a slight red-shift in the region of 200–350 nm upon increasing the doping concentration (Fig. S3 in Supporting information). Meanwhile, the fluorescence and RTP properties of the PVA-Tpy-derivatives (0.025–0.4 wt%) films were systematically investigated (Figs. S4 and S5 in Supporting information). Except for the appearance of new emission band of PVA-Tpy-NH_2 film at 0.4 wt%, the position of prompt emission of composite films almost remains unchanged upon increasing doping concentration from 0.025 wt% to 0.4 wt% (Fig. S4). The RTP emission of PVA-Tpy-COOH is enhanced when the doping concentration increases (Fig. S5a). However, the RTP intensity of PVA-Tpy-NH_2 undergoes a consecutive decrease with an apparent redshift (Fig. S5c). Both the PVA-Tpy-Ph–COOH and PVA-Tpy-Ph–NH_2 films manifest an optimal doing concentration is 0.1 wt%, demonstrating the strongest RTP emission (Figs. S5b and d). Therefore, we select RTP films with doping concentration of 0.1 wt% for following pH-responsiveness studies.

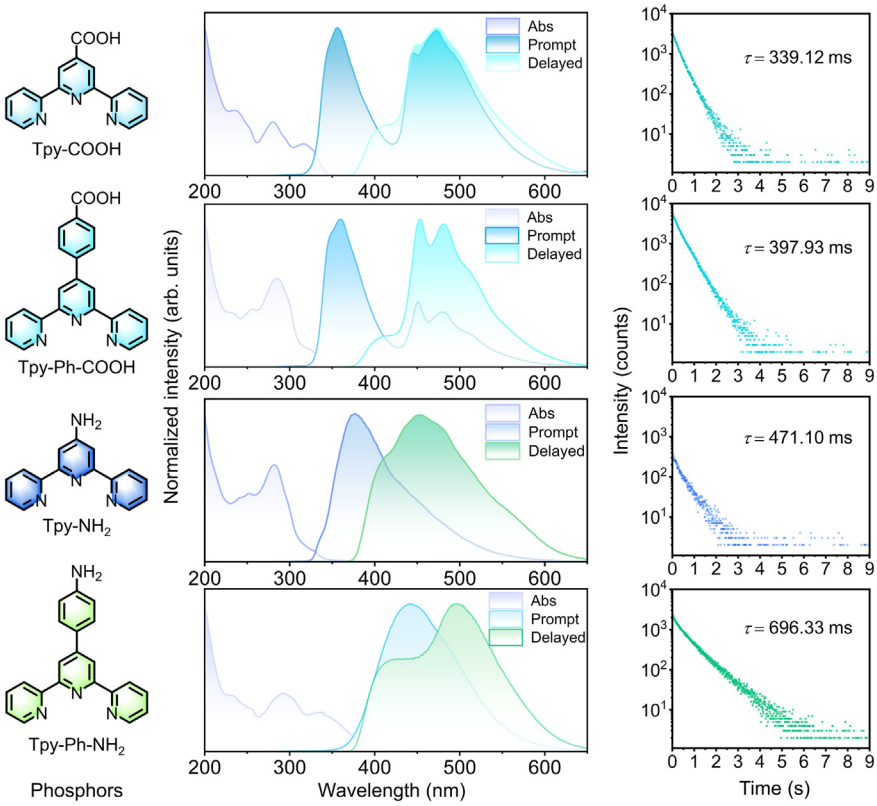

Fig. 1. The molecular structures of organic phosphors (Tpy-COOH, Tpy-Ph–COOH, Tpy-NH_2, and Tpy-Ph–NH_2), and UV absorbance, prompt and delayed-steady photoluminescence spectra and time-resolved emission-decay profiles of corresponding RTP films ($\lambda_{ex} = 254$ nm, $c = 0.1$ wt%).

To study the chemical composition and hydrogen bonding interactions of the PVA-Tpy derivatives, attenuated total reflectance-Fourier transform infrared (ATR-FTIR) spectroscopy and powder X-ray diffraction (XRD) were thoroughly carried out. Due to the low doping concentration, the vibration absorption peak of Tpy derivatives can hardly be observed in the ATR-FTIR spectra (Fig. S6 in Supporting information). However, the stretching absorption of the hydroxyl group (−OH) is distinctly shifted to lower frequency upon increasing the doping concentrations, indicating strong hydrogen bonding interactions between PVA chains and Tpy dericatives. Taking PVA-Tpy-COOH films for examples, the absorption peak at 3274 cm^{-1} for −OH of pure PVA eventually shifts to 3262 cm^{-1} for PVA-Tpy-COOH (0.4 wt%). Besides, XRD patterns of these composite RTP films display a similar wide peak at around 20°, indicating the semi-crystalline state of PVA matrix remains unchanged after the introduction of Tpy derivatives (Fig. S7 in Supporting information). Taken together, the multiple hydrogen bonding interactions and the rigid quenchers barrier provided by PVA matrix should be responsible for the ultralong RTP emission of these composite films.

In addition to the above optical regulation by modifying carboxyl or amino group, the Tpy unit provides an excellent platform for pH stimuli-responsiveness. Interestingly, the PVA-Tpy-COOH film exhibit less sensitive to HCl and NaOH (50-fold), showing almost slight change in both prompt and delayed emission (Figs. 2a and e). Although the spectra of PVA-Tpy-NH_2 film have no obvious change upon exposure to 50 molar equivalents of NaOH, it undergoes obvious variations in emission spectra after acid treatment, revealing an appearance of new fluorescence emission band at around 350 nm and significant red-shifts from 450 nm to 550 nm for delayed emission (Figs. 2c and g). Strikingly, both PVA-Tpy-Ph–COOH and PVA-Tpy-Ph–NH_2 films display obvious changes upon exposure to HCl and NaOH, demonstrating significant reductions in prompt and delayed emission intensity (Figs. 2b, d, f and h).

To further elucidate the effect of molar equivalent of acid and base on the RTP performance, the composite RTP films were treated with a series of acid and base with specific equivalent gradients (10-, 50-, 100-fold). As shown in the Figs. 3a-d and Table S1 (Supporting information), the phosphorescence lifetimes of almost all RTP films are shortened upon exposure to HCl. Except for PVA-Tpy-COOH film, the afterglow emission of PVA-Tpy-Ph–COOH, PVA-Tpy-NH_2, and PVA-Tpy-Ph–NH_2 films was quenched after treated with 50 molar equivalents of HCl. Particularly, PVA-Tpy-COOH film still has a lifetime of 329.64 ms when exposed to 50 molar equivalents of HCl, in addition to fully quenching of afterglow emission in the case of 100-fold HCl treatment. On the contrary, the lifetimes of PVA-Tpy-COOH, PVA-Tpy-Ph–COOH and PVA-Tpy-Ph–NH_2 films show a slight prolongation upon base treatments. The lifetimes elongation is mainly attributed to increasing crystallinity of PVA after being immersed into a solution of NaOH [59]. The RTP properties can be improved by such a more rigid microenvironment. While no obvious change can be observed for PVA-Tpy-NH_2 film upon exposure to NaOH. The photos of these composite RTP films before and after acid or base treatment are consistent with the corresponding variation of lifetimes (Fig. 3e).

To figure out the largely diminished afterglow emission upon acid treatment, ^{1}H NMR spectra of Tpy-COOH were recorded before and after exposure to HCl. As displayed in Fig. S10 (Supporting information), all hydrogen atoms show down field shifts ($\Delta\delta = 0.17$ and 0.25 ppm for Tpy-$H^{3,3''}$ and Tpy-$H^{5,5''}$, respectively) upon the addition of excessive HCl, implying the loss of electron density due to protonation of Tpy unit. That is, the diminution of RTP emission and shortened lifetime may be ascribed to protonation of Tpy. If

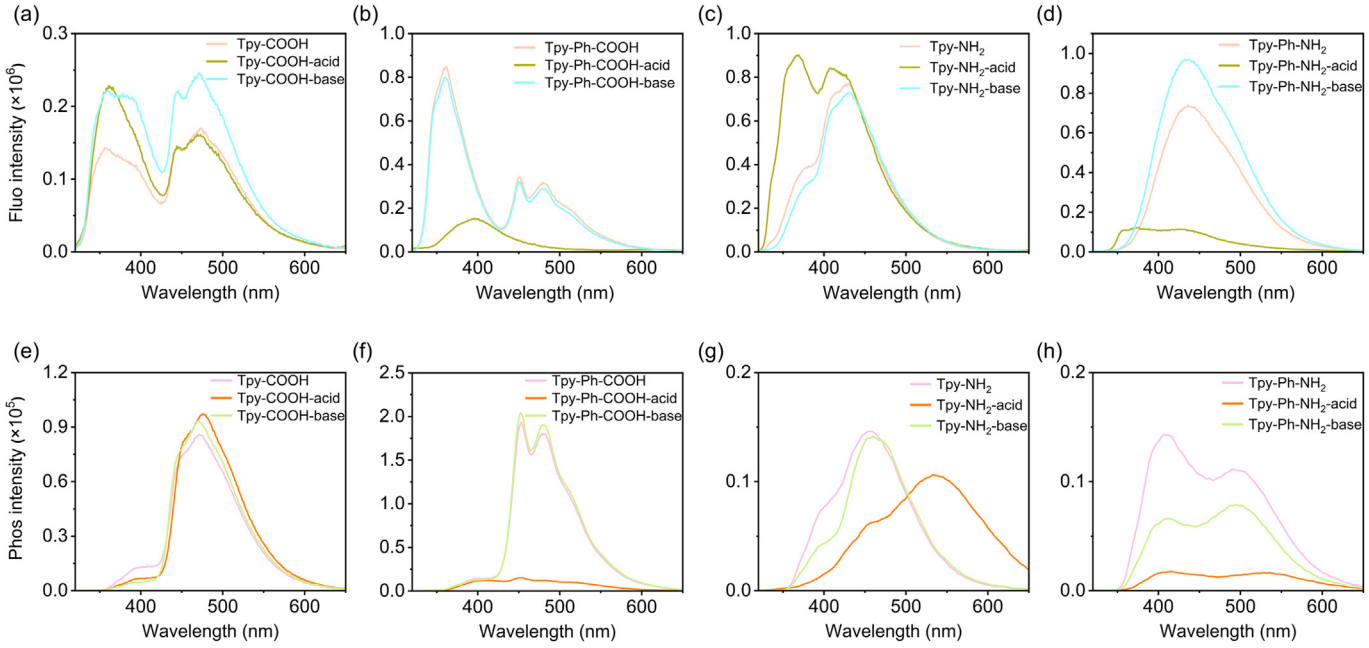

Fig. 2. (a-d) Prompt emission spectra of PVA-Tpy-COOH, PVA-Tpy-Ph–COOH, PVA-Tpy-NH_2, and PVA-Tpy-Ph–NH_2 before and after acid-treatment and base-treatment, respectively ($\lambda_{ex} = 254$ nm, 50 molar equivalents of HCl and NaOH were used, $c = 1.0$ mol/L). (e-h) Delayed emission spectra of PVA-Tpy-COOH, PVA-Tpy-Ph–COOH, PVA-Tpy-NH_2, and PVA-Tpy-Ph–NH_2 before and after acid-treatment and base-treatment, respectively ($\lambda_{ex} = 254$ nm, 50 molar equivalents of HCl and NaOH were used, $c = 1.0$ mol/L).

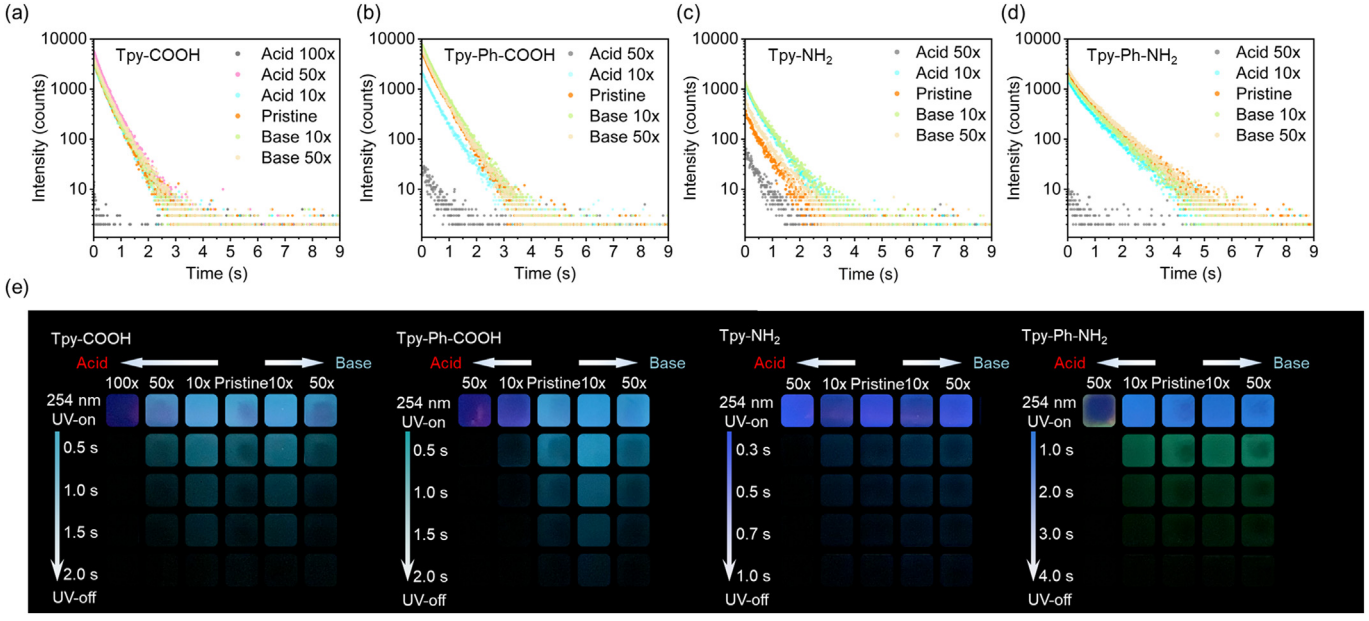

Fig. 3. (a-d) Time-resolved emission-decay profiles of PVA-Tpy-COOH, PVA-Tpy-Ph–COOH, PVA-Tpy-NH_2, and PVA-Tpy-Ph–NH_2 films before and after acid-treatment and base-treatment, respectively (10, 50, 100 molar equivalents of HCl and NaOH were used, $c = 1.0$ mol/L). (e) Photographs of PVA-Tpy-COOH, PVA-Tpy-Ph–COOH, PVA-Tpy-NH_2, and PVA-Tpy-Ph–NH_2 films before and after acid-treatment and base-treatment, respectively (10, 50, 100 molar equivalents of HCl and NaOH were used, $c = 1.0$ mol/L), the photos were taken under 254 nm UV excitation and at different time intervals after the removal of UV irradiation.

so, such afterglow quenching should be restored by deprotonation. Indeed, the emission performance of PVA-Tpy-COOH film is recovered after being immersed into the NaOH solution (2×10^{-3} mol/L) for 20 min, and followed by thorough evaporation at 80 °C for 1.0 h (Fig. 4). As shown in Fig. 4a, the restored PVA-Tpy-COOH film reveals ultralong RTP feature with afterglow lasting for about 2 s after the removal of excitation source. Accordingly, both fluorescence and phosphorescence emission at 470 nm are reemerged (Figs. 4b and c), indicating the reversible pH stimuli-responsiveness of the Tpy-derivatives-based RTP films.

Encouraged by the excellent optical properties and satisfactory pH-responsiveness of these Tpy-derivatives-based RTP films, we developed spatial-time-resolved anti-counterfeiting applications. As a proof-of-concept, an anti-counterfeiting pattern consisting of fireworks barrel was designed and fabricated by using pristine and acid-treated PVA-Tpy-Ph–NH_2 precursor solutions as paints (Fig. 5a), considering the longest afterglow duration and obvious recession in RTP performance after acid-treatment of PVA-Tpy-Ph–NH_2. Interestingly, the anti-counterfeiting pattern displayed cyan fluorescence emission under 254 nm UV light along

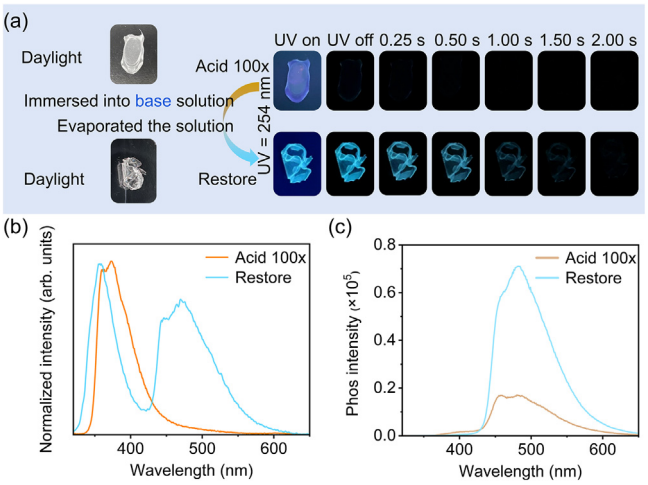

Fig. 4. The illustration of RTP recovery of acid-treated PVA-Tpy-COOH films by the addition of base. (a) Photographs of acid-treated and restored PVA-Tpy-COOH films under daylight, 254 nm UV excitation and at different time intervals after the removal of UV irradiation. (b, c) Prompt and delayed emission spectra of acid-treated and restored PVA-Tpy-COOH films.

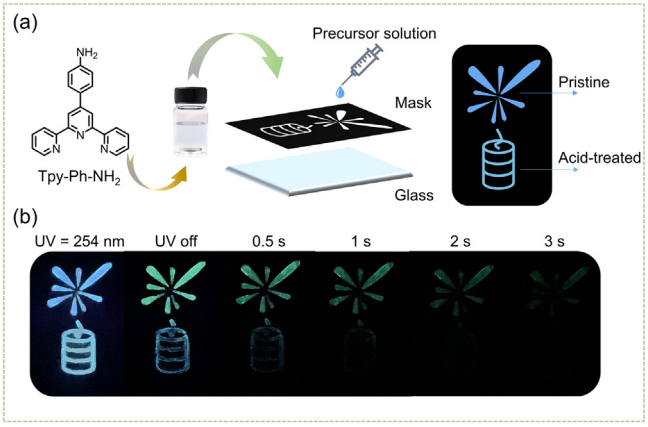

Fig. 5. The spatial-time-resolved anti-counterfeiting application. (a) The schematic illustration of designing and fabricating anti-counterfeiting by using pristine and acid-treated PVA-Tpy-Ph–NH_2 precursor solutions as paints. (b) Photographs of the anti-counterfeiting pattern under 254 nm UV excitation and at different time intervals after the removal of UV irradiation.

with fading out after erasing UV irradiation (Fig. 5b). Due to shortened lifetime of acid-treated PVA-Tpy-Ph–NH_2 material, the part of fireworks barrel disappeared faster than fireworks part, fading out in 1.0 s. Intense green afterglow can be observed in the fireworks part, lasting for about 3 s. With no doubt, such spatial-time-resolved variations of anti-counterfeiting pattern greatly improves information security for verifying the authenticity of commodities.

In summary, we have presented a feasible strategy for achieving pH-responsive RTP materials by the introduction of Tpy derivatives into PVA matrix. The Tpy derivatives-based films display excellent RTP performance with longest lifetime of up to 696.33 ms, providing excellent platforms for studying the pH-responsiveness. Strikingly, the RTP performance undergoes a significant degradation upon exposure to acid, which can be attributed to protonation of Tpy units. Although no obvious change can be observed for PVA-Tpy-Ph–COOH, PVA-Tpy-NH_2 films upon exposure to NaOH, the lifetimes of PVA-Tpy-COOH and PVA-Tpy-Ph–NH_2 films show a slight prolongation upon base treatments. It can be concluded that the substituent groups play important role in the sensitivity of pH-responsiveness of these Tpy derivatives-based RTP films. Based on the satisfactory RTP emission and pH-responsiveness of these RTP films, spatial-time-resolved anti-counterfeiting application was successfully established for enhancing the security level. This study not only offers a reliable strategy for developing smart RTP materials but also paves a new avenue to improve the security level of anti-counterfeiting applications.

Declaration of competing interest

The authors declare that they have no known competing financial interests or personal relationships that could have appeared to influence the work reported in this paper.

CRediT authorship contribution statement

Jiayin Zhou: Writing – original draft, Visualization, Validation, Software, Methodology, Investigation, Formal analysis, Data curation. **Depeng Liu:** Visualization, Validation, Resources, Methodology, Investigation, Data curation. **Longqiang Li:** Validation, Investigation. **Min Qi:** Visualization, Validation. **Guangqiang Yin:** Writing – review & editing, Supervision, Project administration, Funding acquisition, Data curation. **Tao Chen:** Writing – review & editing, Supervision, Project administration, Funding acquisition, Conceptualization.

Acknowledgments

This project was financially supported by the National Natural Science Foundation of China (No. 22205249), Zhejiang Provincial Natural Science Foundation of China (No. LQ23B040002), the Sino-German Mobility Program (No. M-0424), Ningbo International Cooperation Project (No. 2023H019), China Postdoctoral Science Foundation (Nos. 2021TQ0341, 2022M723252). We also thank Prof. Patrick Théato from the Karlsruhe Institute of Technology for his thoughtful suggestions.

Supplementary materials

Supplementary material associated with this article can be found, in the online version, at doi:10.1016/j.cclet.2024.109929.

References

[1] W. Zhao, Z. He, B.Z. Tang, Nat. Rev. Mater. 5 (2020) 869–885.
[2] S. Xu, R. Chen, C. Zheng, W. Huang, Adv. Mater. 28 (2016) 9920–9940.
[3] H. Shi, W. Yao, W. Ye, et al., Acc. Chem. Res. 55 (2022) 3445–3459.
[4] Q. Liao, Q. Li, Z. Li, Adv. Mater. (2023), doi:10.1002/adma.202306617.
[5] T. Zhang, X. Ma, H. Wu, et al., Angew. Chem. Int. Ed. 59 (2020) 11206–11216.
[6] G. Yin, J. Zhou, W. Lu, et al., Adv. Mater. (2024), doi:10.1002/adma.202311347.
[7] Q. Li, Y. Tang, W. Hu, Z. Li, Small 14 (2018) e1801560.
[8] X. Ma, J. Wang, H. Tian, Acc. Chem. Res. 52 (2019) 738–748.
[9] X.K. Ma, Y. Liu, Acc. Chem. Res. 54 (2021) 3403–3414.
[10] E. Middha, B. Liu, ACS Nano 14 (2020) 9228–9242.
[11] B. Zhou, D. Yan, Adv. Funct. Mater. 33 (2023) 2300735.
[12] S.K. Lower, M.A. El-Sayed, Chem. Rev. 66 (1966) 199–241.
[13] H. Zhu, I. Badía-Domínguez, B. Shi, et al., J. Am. Chem. Soc. 143 (2021) 2164–2169.
[14] W. Li, Q. Huang, Z. Mao, et al., Nat. Commun. 13 (2022) 7423.
[15] S. Garain, S.N. Ansari, A.A. Kongasseri, et al., Chem. Sci. 13 (2022) 10011–10019.
[16] L. Gu, H. Wu, H. Ma, et al., Nat. Commun. 11 (2020) 944.
[17] X. Ma, C. Xu, J. Wang, H. Tian, Angew. Chem. Int. Ed. 57 (2018) 10854–10858.
[18] H. Peng, G. Xie, Y. Cao, et al., Sci. Adv. 8 (2022) eabk2925.
[19] H. Gao, X. Ma, Aggregate 2 (2021) e38.
[20] J. Han, W. Feng, D.Y. Muleta, et al., Adv. Funct. Mater. 29 (2019) 1902503.
[21] Y. Wang, J. Yang, M. Fang, et al., Matter 3 (2020) 449–463.
[22] H. Sun, L. Zhu, Aggregate 4 (2023) e253.
[23] Y. Su, S.Z.F. Phua, Y. Li, et al., Sci. Adv. 4 (2018) eaas9732.
[24] L. Ma, S. Sun, B. Ding, et al., Adv. Funct. Mater. 31 (2021) 2010659.
[25] R. Tian, S.M. Xu, Q. Xu, C. Lu, Sci. Adv. 6 (2020) eaaz6107.
[26] G. Qu, Y. Zhang, X. Ma, Chin. Chem. Lett. 30 (2019) 1809–1814.
[27] Y. Zhang, Y. Su, H. Wu, et al., J. Am. Chem. Soc. 143 (2021) 13675–13685.
[28] G. Jiang, J. Yu, J. Wang, B.Z. Tang, Aggregate 3 (2022) e285.
[29] Q. Li, Z. Li, Acc. Chem. Res. 53 (2020) 962–973.
[30] J. Yang, M. Fang, Z. Li, Aggregate 1 (2020) 6–18.
[31] G. Yin, W. Lu, J. Huang, et al., Aggregate 4 (2023) e344.

[32] G. Yin, G. Huo, M. Qi, et al., Adv. Funct. Mater. 34 (2023) 2310043.
[33] S. Cai, H. Shi, Z. Zhang, et al., Angew. Chem. Int. Ed. 57 (2018) 4005–4009.
[34] E. Hamzehpoor, C. Ruchlin, Y. Tao, et al., Nat. Chem. 15 (2023) 83–90.
[35] S. Liu, Y. Lin, D. Yan, Chin. Chem. Lett. 34 (2023) 107952.
[36] J. Yang, M. Fang, Z. Li, Acc. Mater. Res. 2 (2021) 644–654.
[37] F. Gu, X. Ma, Chem. Eur. J. 28 (2022) e202104131.
[38] L. Huang, C. Qian, Z. Ma, Chem. Eur. J. 26 (2020) 11914–11930.
[39] J. Yang, M. Fang, Z. Li, InfoMat 2 (2020) 791–806.
[40] L. Tu, Y. Chen, X. Song, et al., Angew. Chem. Int. Ed. (2024), doi:10.1002/anie.202402865.
[41] Y. Tian, Y. Gong, Q. Liao, et al., Cell Rep. Phys. Sci. 1 (2020) 100052.
[42] L. Huang, B. Chen, X. Zhang, et al., Angew. Chem. Int. Ed. 57 (2018) 16046–16050.
[43] J. Xu, H. Feng, H. Teng, et al., Chem. Eur. J. 24 (2018) 12773–12778.
[44] R. Liu, B. Ding, D. Liu, X. Ma, Chem. Eng. J. 421 (2021) 129732.
[45] S. Sun, L. Ma, J. Wang, et al., Natl. Sci. Rev. 9 (2022) nwab085.
[46] G. Wang, Z. Wang, B. Ding, X. Ma, Chin. Chem. Lett. 32 (2021) 3039–3042.
[47] J. Yang, X. Zhen, B. Wang, et al., Nat. Commun. 9 (2018) 840.
[48] X. Jia, C. Shao, X. Bai, et al., Proc. Natl. Acad. Sci. U. S. A. 116 (2019) 4816–4821.
[49] Z. Chai, C. Wang, J. Wang, et al., Chem. Sci. 8 (2017) 8336–8344.
[50] Q. Wu, H. Ma, K. Ling, et al., ACS Appl. Mater. Interfaces 10 (2018) 33730–33736.
[51] D. Li, Y. Yang, J. Yang, et al., Nat. Commun. 13 (2022) 347.
[52] H. Wu, L. Gu, G.V. Baryshnikov, et al., ACS Appl. Mater. Interfaces 12 (2020) 20765–20774.
[53] Z. Mao, Z. Yang, Y. Mu, et al., Angew. Chem. Int. Ed. 54 (2015) 6270–6273.
[54] H. Wu, P. Zhao, X. Li, et al., ACS Appl. Mater. Interfaces 9 (2017) 3865–3872.
[55] L. Huang, L. Liu, X. Li, et al., Angew. Chem. Int. Ed. 58 (2019) 16445–16450.
[56] G.A. Filonenko, J.R. Khusnutdinova, Adv. Mater. 29 (2017) 1700563.
[57] Y. Gong, G. Chen, Q. Peng, et al., Adv. Mater. 27 (2015) 6195–6201.
[58] G. Yin, J. Huang, D. Liu, et al., Chin. Chem. Lett. 34 (2023) 107290.
[59] M.A. Darabi, A. Khosrozadeh, Y. Wang, et al., Adv. Sci. 7 (2020) 1902740.